The elongated ciliated cells derived from nasal polyps are distinctly different from ciliated cells in different parts of the nasal mucosa

Huiyi Deng*, Mingrui Pan*, Qintai Yang#, Huijun Qiu#

Rhinology 64: 4, 0 - 0, 2026
https://doi.org/10.4193/Rhin25.225

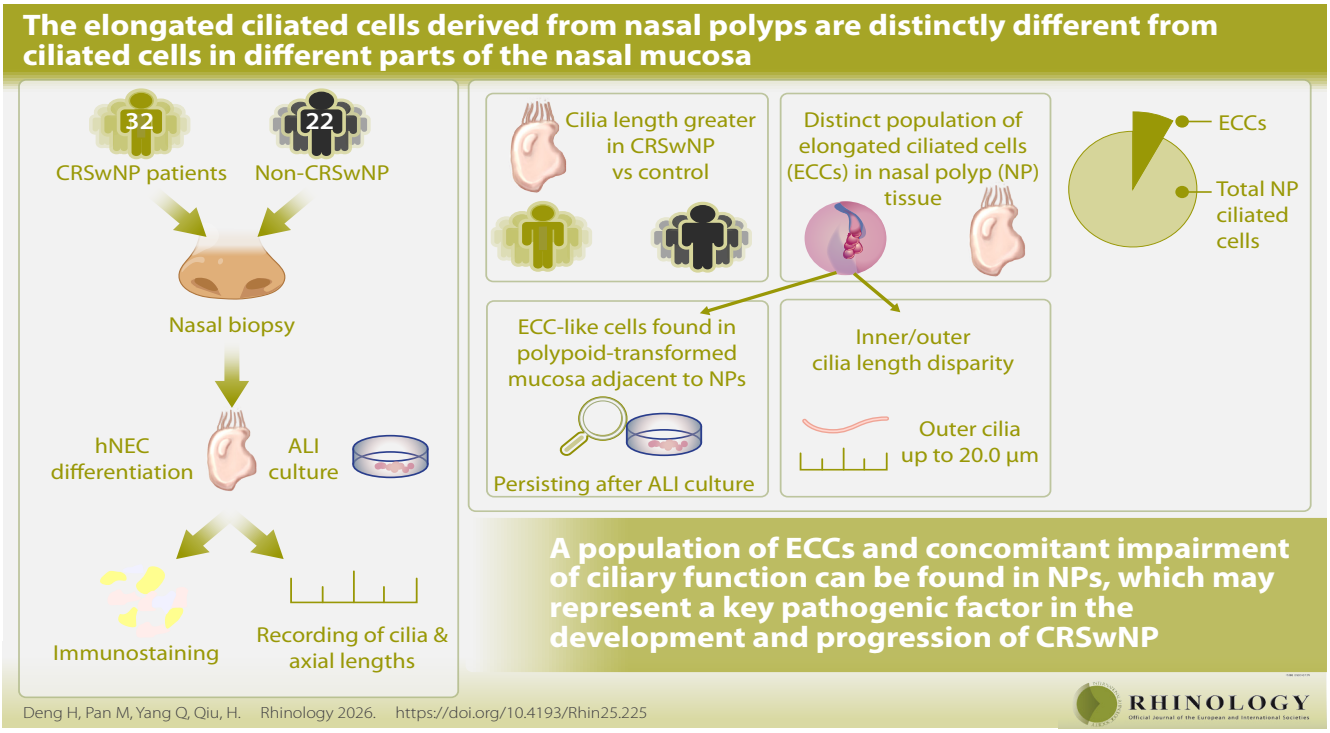

Abstract

Background: Ciliary abnormalities are implicated in the pathogenesis of chronic rhinosinusitis with nasal polyps (CRSwNP), but whether these changes are site-specific traits or confined to specific cell populations remains unknown. Here, we systematically examined ciliated cells throughout the sinonasal tract to characterize disease-specific ciliary alterations and identify a distinct population of elongated ciliated cells in nasal polyps (NPs).

Methods: Nasal biopsy specimens were obtained from patients with CRSwNP (n=32) and non-CRSwNP (n=22). hNECs were differentiated at the air-liquid interface (ALI). Tissue sections, cytospin preparations, and ALI cultures were immunostained for α-tubulin. Cilia length, length of horizontal axis, and length of vertical axis of ciliated cells were recorded.

Results: Cilia length was significantly greater in CRSwNP patients than in non-CRSwNP controls (8.17 ± 3.35 µm vs. 5.67 ± 1.64 µm). Within NPs tissues, we identified a distinct population of elongated ciliated cells (ECCs) exhibiting marked inner/outer cilia length disparity, with outer cilia reaching up to 20.0 µm. These ECCs accounted for 8.10% ± 3.56% of total ciliated cells in NPs. Notably, ECCs-like cells were also detected in polypoid-transformed mucosa adjacent to NPs and persisted after ALI culture. In contrast, ciliated cell dimensions did not differ between groups or across the nasal anatomical sites examined.

Conclusion: A population of ciliated cells characterized by abnormally elongated cilia and concomitant impairment of ciliary function can be found in NPs, which may represent a key pathogenic factor in the development and progression of CRSwNP.

Key words: cilia, chronic rhinosinusitis with nasal polyps, elongated ciliated cells, human nasal epithelial cells, nasal epithelium

Corrected Proof

Introduction

The nasal mucosa is constantly exposed to harmful substances and relies on mucociliary clearance (MCC), the respiratory system's primary innate defense [1] involving cilia and mucus production [2,3]. In chronic rhinosinusitis with nasal polyps (CRSwNP), cilia and ciliated cell damage impairs MCC [4], leading to mucus stasis, secondary infection, and persistent inflammation that perpetuate the disease process [2]. Consequently, patients experience prolonged symptoms such as congestion, rhinorrhea, facial pain, and reduced smell [5], significantly compromising their quality of life and productivity [6] while imposing a substantial economic burden [7].

The mechanism underlying this pathological MCC remains unclear. Each ciliated cell bears 50–200 cilia (5.0–7.0 µm long, 0.2–0.3 µm wide) [8]. Prior research noted ectopic ciliary elongation in nasal polyps (NPs) tissue compared to the inferior turbinate, but did not examine other regions of the nasal cavity and sinuses [9]. The study raises a key unresolved question of whether elongation is a site-specific trait (e.g., of the ostiomeatal complex) or intrinsic to NPs tissue itself. A comprehensive analysis of the nasal cavity and sinuses mucosa is needed to determine if ciliary abnormalities are uniform or region-specific in CRSwNP. This study systematically compared ciliary morphology across multiple nasal subsites and NPs tissue, focusing on disease-related structural changes. This comprehensive mapping of cilia distribution across the nasal cavity and sinuses establishes a spatial framework for understanding region-specific contributions to cilia-driven pathology in CRSwNP.

Materials and methods

Subjects and sample collection

Nasal mucosal biopsies were collected from CRSwNP and non-CRSwNP patients during endoscopic sinus surgery (ESS) at The Third Affiliated Hospital of Sun Yat-sen University in 2024 (Table 1). The study was approved by the hospital's ethics committee (Approval No. RG2023-124-01). The diagnosis of CRSwNP was established according to the criteria outlined in the European Position Paper on Rhinosinusitis and Nasal Polyps (EPOS) 2020[5]. For more detailed experimental procedures, see Supplementary Material.

Human nasal epithelial cell culture

Human nasal epithelial cells (hNECs) were isolated from fresh nasal specimens and cultured in a progenitor cell culture system, as previously reported [10]. Subsequently, they were transferred to an air-liquid interface (ALI) system, where they matured into cells with cilia within four weeks [10].

Cytospin preparation

Cytospin slides were prepared by centrifuging cells onto glass slides to preserve cellular morphology for imaging [11]. Based on our previous report [10], hNECs were dissociated by trypsinization and fixed. Cytospin slides (2×10^4 cells/slide) were prepared by spinning for five minutes at 500 rev/min on a Shandon Cytospin 4 Cytocentrifuge (Thermo Fisher Scientific, Waltham, MA, USA).

Immunofluorescent staining

Immunofluorescent (IF) staining was performed as previously reported [10]. Paraffin sections were baked at 64°C for two hours, deparaffinized in xylene and gradient alcohol, and subjected to antigen retrieval in Tris-EDTA buffer at 100°C for ten minutes. After cooling, samples were blocked with 10% goat serum for 30 minutes and permeabilized with 0.1% Triton X-100. Primary antibody against α-tubulin (1:400; Cat# ab24610; Abcam, Cambridge, UK) was applied overnight at 4°C, followed by incubation with Alexa Fluor 488-conjugated secondary antibody (Thermo Fisher Scientific, Waltham, MA, USA) for one hour at room temperature.

Measurement of cilia and cellular morphology

ImageJ (v1.8.0.345; NIH, Bethesda, MD, USA) was used to measure cell cilia length (performed as previously reported [10]), the length of the cell parallel to the direction of cilia growth (defined as the horizontal axis, lengthHA), and the length of the cell central perpendicular to the direction of cilia growth (defined as the vertical axis, lengthVA). Ten ciliated cells were examined per cytospin sample; therefore, the total number of cells analyzed was ten times the sample size. For more detailed experimental procedures, see Supplementary Material.

Statistics and reproducibility

All statistical analyses were performed using SPSS (version 29.0.2.0; IBM Corp., Armonk, NY, USA), and graphs were generated using GraphPad Prism (version 8.0; GraphPad Software, San Diego, CA, USA). Based on preliminary data, a sample size of 19–32 per group provided >80% power to detect a mean difference of 2.5 µm in cilia length with $\alpha = 0.05$. Between-group comparisons were performed using an unpaired Student's t-test (for two groups) or one-way ANOVA (for three or more groups). Results were reported as mean differences with 95% confidence intervals. When significant differences were found in multiple group comparisons, post-hoc pairwise tests with Bonferroni correction were conducted. A two-tailed P value of < 0.05 was considered statistically significant.

Results

Regional heterogeneity of nasal ciliary morphology

To investigate regional differences in ciliary morphology across the nasal cavity and sinuses, we performed IF staining for α-tubulin, a validated structural marker of the ciliary axoneme [10,12], on samples from multiple anatomical sites. These included the ostiomeatal complex (OMC; comprising the middle turbina-

Corrected Proof

Table 1. Baseline characteristics of study participants.

mucosa types	disease type	cases	age (y)	sex (male)	smoking exposure	patients with atopy	L-M sinus CT score	EosCRSwNP
nasal polyps	CRSwNP	19	42.42±16.78	13 (68.4%)	4 (21.1%)	5 (26.31%)	14.21±6.06	5 (26.3%)
frontal sinus	CRSwNP	0	-	-	-	-	-	-
	non-CRSwNP	2	29.50±2.12	2 (100%)	1 (50%)	0 (0%)	16.50±4.95	-
ethmoid sinus	CRSwNP	5	47.20±20.07	2 (40%)	2 (40%)	1 (20%)	14.60±4.04	2 (40%)
	non-CRSwNP	4	30.00±3.16	4 (100%)	1 (25%)	1 (25%)	14.00±6.68	-
sphenoid sinus	CRSwNP	4	46.75±22.69	3 (75%)	1 (25%)	2 (50%)	17.00±5.94	4 (100%)
	non-CRSwNP	1	39	1 (100%)	1 (100%)	0 (0%)	3	-
maxillary sinus	CRSwNP	7	44.29±13.60	4 (57.1%)	2 (28.6%)	2 (28.57%)	10.43±4.93	3 (42.9%)
	non-CRSwNP	1	28	1 (100%)	0 (0%)	0 (0%)	13	-
unicate process	CRSwNP	5	47.20±16.18	1 (20%)	0 (0%)	0 (0%)	8.60±5.46	1 (20%)
	non-CRSwNP	5	39.00±11.11	4 (80%)	1 (20%)	0 (0%)	6.80±3.49	-
ethmoid bulla	CRSwNP	4	42.75±12.42	3 (75%)	0 (0%)	1 (25%)	14.25±7.27	3 (75%)
	non-CRSwNP	1	29	0 (0%)	0 (0%)	0 (0%)	11	-
superior turbinate	CRSwNP	2	39.50±24.75	0 (0%)	0 (0%)	0 (0%)	18.50±0.71	1 (50%)
	non-CRSwNP	1	74	0 (0%)	0 (0%)	0 (0%)	8	-
middle turbinate	CRSwNP	3	40.33±17.56	1 (33.3%)	0 (0%)	0 (0%)	14.33±7.23	1 (33.3%)
	non-CRSwNP	4	43.25±16.26	2 (50%)	0 (0%)	1 (25%)	7.25±5.74	-
inferior turbinate	CRSwNP	2	49.50±10.61	1 (50%)	0 (0%)	0 (0%)	12.00±8.49	1 (50%)
	non-CRSwNP	3	42.33±8.74	3 (100%)	1 (33.33%)	1 (33.33%)	7.33±7.02	-
total	CRSwNP	32	44.97±15.42	15 (46.9%)	5 (15.6%)	6(18.75%)	13.06±5.86	16 (50%)
	non-CRSwNP	22	38.36±12.95	15 (68.18%)	5 (22.73%)	3 (13.64%)	9.50±5.83	-

Data are presented as mean ± SD or number (percentage), as appropriate. Specifically, continuous variables (including age and Lund-Mackay scores) are reported as mean ± SD. Other categorical variables are shown as counts with percentages. Eosinophilic chronic rhinosinusitis with nasal polyps (eosCRSwNP) was defined by an eosinophil count exceeding 10 per high-power field (HPF; 400× magnification). Eosinophil counts were performed on 10 randomly selected HPFs per specimen, and the mean count was used for diagnosis.

te, uncinate process, ethmoid bulla, frontal sinus, ethmoid sinus and maxillary sinus) as well as other nasal regions (superior turbinate, inferior turbinate and sphenoid sinus). Ciliary morphology was characterized by quantifying cilia length and cellular dimensions (lengthHA and lengthVA; Figure 1A). Tissue sections showed that the ciliated epithelium of the nasal mucosa was continuous and structurally intact across all sampled sites, with no significant regional differences in ciliary length or distribution (Figure 1B). Cytospin slides were largely consistent with these findings (Figure 1C), indicating that the processing method did not introduce notable morphological alterations; additionally, cytospin allowed clearer visualization of the complete outline of individual ciliated cells. Observation of hNECs revealed that the cells were oval-shaped, with cilia distributed at one end of the cell, away from the nucleus, in a fan-like pattern with uniform length and density. In contrast, cilia from inferior turbinate cells appeared straighter, whereas those from other nasal sites frequently exhibited curling or irregular bending at their distal ends (Figure 1).

Ciliary elongation distinguishes nasal polyps epithelium from adjacent nasal mucosa

Building on this regional heterogeneity, we next quantified ciliary characteristics in three groups. Cilia length, $length_{VA}$, $length_{HA}$, and their ratios were measured in three groups: NPs tissues from CRSwNP patients, other-site nasal mucosa from CRSwNP patients, and nasal mucosa from non-CRSwNP patients. Relative to NPs tissues, cilia length was significantly shorter in non-CRSwNP mucosal sites (5.67 ± 1.64 μm vs 8.17 ± 3.35 μm, Table 2), particularly in the uncinate process, ethmoid sinus, maxillary sinus, middle turbinate, and inferior turbinate. Similarly, the cilia length of ciliated cells in other parts of CRSwNP patients was also shorter than that from NPs, and the difference was significant in uncinate process (6.54 ± 1.94 μm) and inferior turbinate (5.87 ± 1.82 μm). Similarly, the ratio of cilia length to lengthVA of ciliated cells in non-CRSwNP patients (0.35 ± 0.13, including uncinate process and inferior turbinate) was smaller than that of ciliated cells in NPs (0.42 ± 0.18), and such differences were observed in ciliated epithelium of nasal mucosa from

Corrected Proof

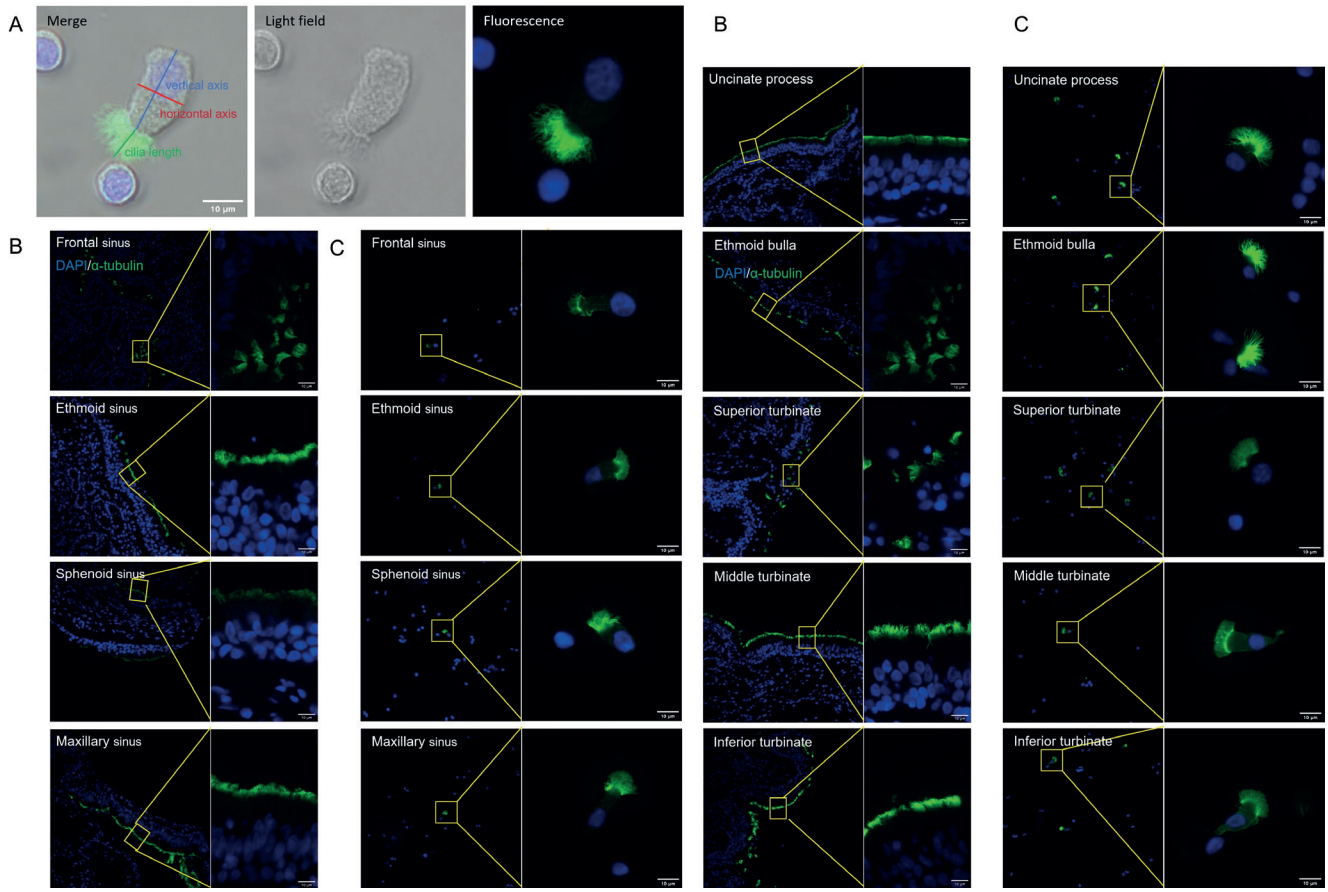

Figure 1. The homogeneity across nasal mucosa by IF staining. (A) Representative images for measurements of horizontal, vertical axis and cilia length for ciliated cells in both light field and IF staining images. (B) IF sections of nasal mucosa tissues and (C) corresponding human nasal epithelial progenitor cells (hNECs) cytospins immunostained with α-tubulin (green) and counterstained with DAPI (blue). Representative IF images from each group are shown (400× magnification, n = 22).

other positions of CRSwNP patients, for example uncinate process (0.30 ± 0.10), maxillary sinus (0.22 ± 0.06) and inferior turbinate (0.28 ± 0.07). No significant differences were observed in the $length_{VA}$, $length_{HA}$ and the ratio of $length_{HA}$ to $length_{VA}$ when comparing the ciliated cells derived from NPs with those from any other mucosa both in non-CRSwNP and CRSwNP, indicating that ciliated cells from different origins maintain similar overall cell size and shape. These findings suggest that the marked ciliary elongation is a distinctive feature of NPs epithelium rather than a general property of all sinonasal mucosa in CRSwNP.

A distinct population of elongated ciliated cells in nasal polyps epithelium exhibits marked ciliary heterogeneity

Within NPs tissues, we identified a distinct subset of ciliated cells exhibiting extreme and spatially partitioned ciliary elongation. These cells, termed elongated ciliated cells (ECCs), displayed individual cilia reaching up to 20.0 μm (Figure 2A). In addition to this length dichotomy, ECCs exhibited marked ciliary heterogeneity, including uneven length distribution, irregular epithelial surface, and disorganized or sparse ciliary alignment (Figure 2B). In contrast, ciliated cells elsewhere in the nasal cavity and sinuses, including the mucosa of all non-polypoid tissues from both CRSwNP and non-CRSwNP groups, displayed uniform cilia lengths of approximately 7.0 μm. IF staining of NPs-derived ciliated cells revealed distinct ciliary stratification. The inner cilia (proximal to the cell body) were short and dense (5.41 ± 1.27 μm), whereas outer cilia exhibited abnormal elongation (15.83 ± 3.43 μm), resulting in a mean outer/inner cilia length ratio of 3.05 ± 0.91 (Figure 2C).

Compared to ciliated cells from non-CRSwNP mucosa and non-polypoid CRSwNP mucosa, the outer cilia of ECCs were significantly longer (Figure 2D). In contrast, the inner cilia of ECCs were significantly shorter; however, no significant difference was observed when compared to non-CRSwNP controls (Figure 2E). Despite these length abnormalities, the cilia length/lengthVA ratio was significantly altered only in outer cilia (0.93 ± 0.25, Figure 2F), not in inner cilia (0.32 ± 0.11, Figure 2G). No significant differences were observed in $length_{VA}$, $length_{HA}$, or the $length_{HA}$/$length_{VA}$ ratio across groups.

Although ECCs were occasionally present in other sinonasal

Corrected Proof

Table 2. Measurements of ciliated cells in nasal polyps and other sinonasal mucosa.

mucosa types	disease types	cases	length of cilia (μm)	ratio of cilia length to lengthVA	lengthVA (μm)	lengthHA (μm)	ratio of lengthHA to lengthVA
nasal polyps	CRSwNP	19	8.17±3.35	0.46±0.21	18.33±3.69	9.11±1.71	0.52±0.14
frontal sinus	CRSwNP	0	-	-	-	-	-
	non-CRSwNP	2	6.33±2.01	0.38±0.14	17.00±2.43	8.52±2.13	0.52±0.17
ethmoid sinus	CRSwNP	5	7.44±2.96	0.45±0.19	16.89±3.35	9.07±1.73	0.56±0.16
	non-CRSwNP	4	5.82±1.46*	0.41±0.16	15.22±3.49	8.34±1.44	0.58±0.15
sphenoid sinus	CRSwNP	4	7.48±3.12	0.47±0.19	16.33±3.70	8.57±1.46	0.55±0.15
	non-CRSwNP	1	6.51±1.26	0.38±0.09	17.24±2.65	8.81±1.41	0.53±0.14
maxillary sinus	CRSwNP	7	7.02±2.98	0.44±20	16.48±3.88	8.46±1.98	0.54±0.17
	non-CRSwNP	1	4.08±0.97	0.22±0.06*	18.83±1.76	8.15±1.27	0.43±0.06*
unicate process	CRSwNP	5	6.54±1.94*	0.37±0.12*	18.75±4.95**	8.76±1.94	0.49±0.13
	non-CRSwNP	5	5.37±1.50**	0.30±0.10***	18.66±4.24	9.02±1.85	0.52±0.18*
ethmoid bulla	CRSwNP	4	7.09±3.93	0.41±0.21	17.72±3.58	9.15±1.89	0.54±0.16
	non-CRSwNP	1	5.37±1.47	0.27±0.08	20.16±4.51	7.73±1.06	0.40±0.12
superior turbinate	CRSwNP	2	7.18±2.73	0.39±0.16	18.46±2.91	8.71±1.78	0.48±0.11
	non-CRSwNP	1	4.75±1.28	0.31±0.09	15.85±2.49	9.86±1.17	0.64±0.13
middle turbinate	CRSwNP	3	6.89±2.59	0.42±0.17	17.14±3.99	9.18±1.40	0.56±0.13
	non-CRSwNP	4	6.71±1.60*	0.43±0.15	16.48±3.52	8.73±2.08*	0.56±0.17
inferior turbinate	CRSwNP	2	5.87±1.82	0.33±0.13	18.72±4.62	8.43±1.66	0.47±0.13
	non-CRSwNP	3	4.79±1.19**	0.28±0.07**	17.33±3.00	9.32±2.60**	0.55±0.15
total	CRSwNP	32	7.00±2.89	0.42±0.18	17.36±4.01	8.78±1.79	0.53±0.16
	non-CRSwNP	22	5.67±1.64***	0.35±0.13***	17.19±3.68	8.77±1.91	0.54±0.16

Data are presented as mean ± SD. p values were calculated using Student's t-test with Bonferroni correction for multiple comparisons. *p < 0.05, **p < 0.01, ***p < 0.001 vs. the nasal polyps group.

regions, comparative analysis revealed significant intergroup differences in the proportion of ECCs to total ciliated cells across all examined regions. The mean percentage of ECCs among total ciliated cells was 8.10% ± 3.55% in NPs, 4.95% ± 3.75% in non-polypoid mucosa from CRSwNP patients, and substantially lower at 1.08% ± 1.37% in mucosa from non-CRSwNP patients (Figure 2H). These findings demonstrate that ECCs are highly enriched in NPs epithelium and suggest that this structurally aberrant ciliary phenotype may contribute to ciliary dysfunction in CRSwNP.

Elongated ciliated cells derived from nasal polyps persist after air-liquid interface culture

Given the susceptibility of mucociliary apparatus to exogenous environmental exposures, including viral pathogens [12] and infectious agents [13], we aimed to investigate whether ECCs still maintain their characteristic stratified elongated architecture when isolated from extrinsic environmental stimuli. Therefore, we cultured hNECs in an in vitro ALI model system to verify whether they retained the intrinsic capacity to preserve their structural integrity. ECCs were still present after a 28-day ALI culture (Figure 2I). The lengths of outer and inner cilia for ECCs of hNECs after ALI culture were 16.50 ± 3.50 μm and 5.66 ± 1.20 μm, respectively. These values were not significantly different from those observed in freshly fixed, tissue-derived ECCs from NPs.

The proportion of ECCs among all ciliated cells after ALI culture was 4.79% ± 1.76%. Although this value was lower than that observed in freshly fixed NPs tissues (8.10% ± 3.55%), the difference did not reach statistical significance. Thus, although a trend toward reduction was observed, the ECCs population remained quantitatively and qualitatively preserved after 28 days of culture. This reduction may reflect a lower proliferative capacity of ECCs during in vitro expansion. These findings demonstrate that the aberrant ciliary phenotype is maintained independently of the native nasal microenvironment, suggesting that this phenotype is an intrinsic property of ECCs independent of the local microenvironment.

Elongated ciliated cells are present in polypoid-transformed nasal mucosa

Corrected Proof

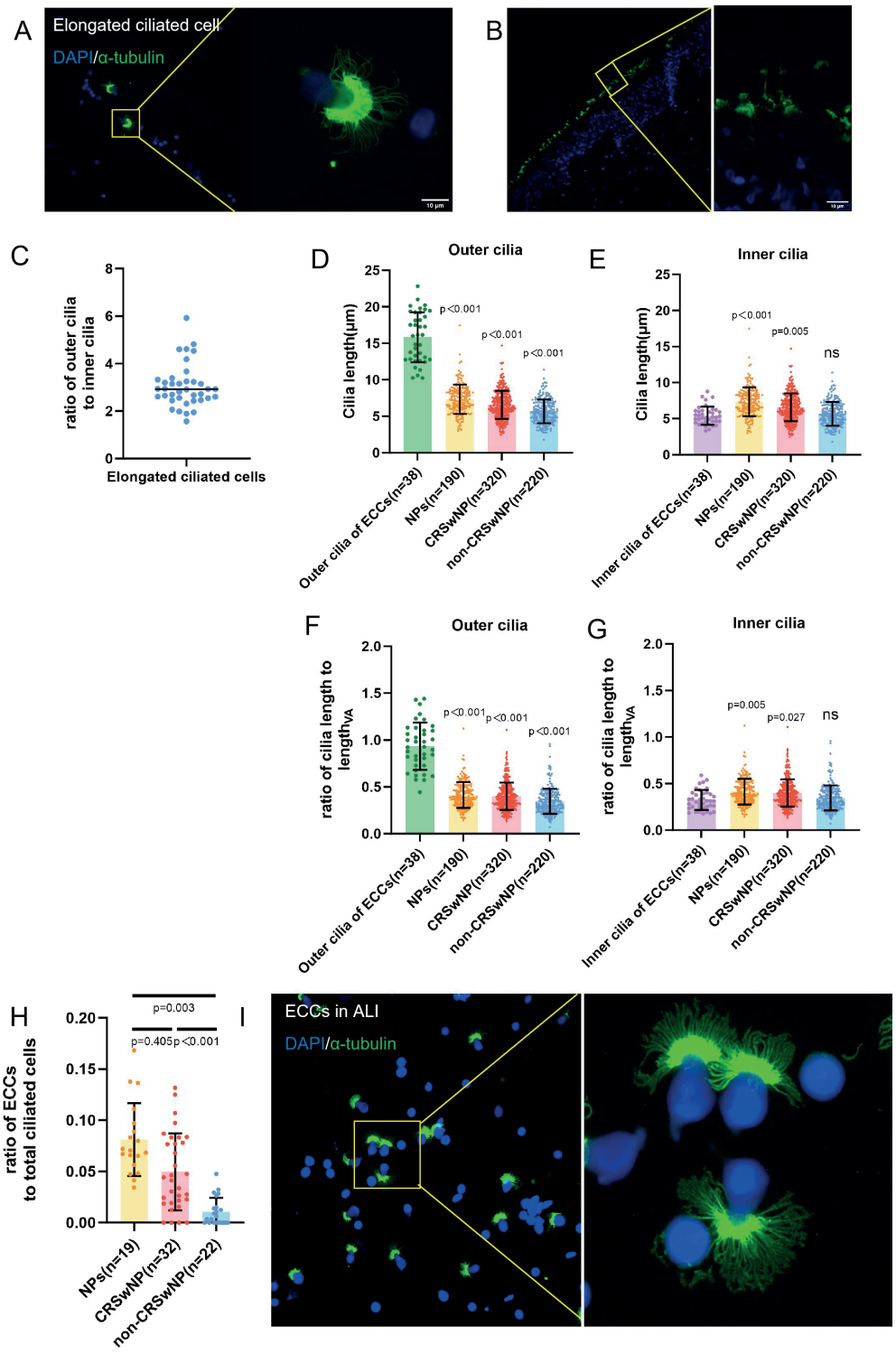

Figure 2. Distinct population of elongated ciliated cells in nasal polyps epithelium exhibits marked intracellular ciliary heterogeneity. (A, B) Representative IF staining images of α-tubulin (green), showing stratified and elongated ciliated cells (ECCs) in cytospin preparations and tissue sections. Nuclei are stained in blue (400× magnification; scale bars = 10 μm). (C) The ratio of the outer cilia length to the inner cilia length within individual ECCs (n = 38). (D, E) Outer (n = 38) and inner cilia of ECCs (n = 38) were each compared for length to unstratified ciliated cells in NPs (n = 190), ciliated cells from other nasal mucosa of CRSwNP patients (n = 320), and those from non-CRSwNP patients (n = 220). (F, G) Outer and inner cilia of ECCs (n = 38) were each compared for the ratio of cilia length to length$_{VA}$ against, unstratified ciliated cells in NPs (n = 190), ciliated cells from other nasal mucosa of CRSwNP patients (n = 320), and those from non-CRSwNP patients (n = 220). (H) Proportion of ECCs among total ciliated cells per microscopic field (n = 19). (I) Representative IF images of α-tubulin (green), showing ECCs after air-liquid interface culture in cytospin preparations. Nuclei are stained in blue (400× magnification; scale bars = 10 μm).

Corrected Proof

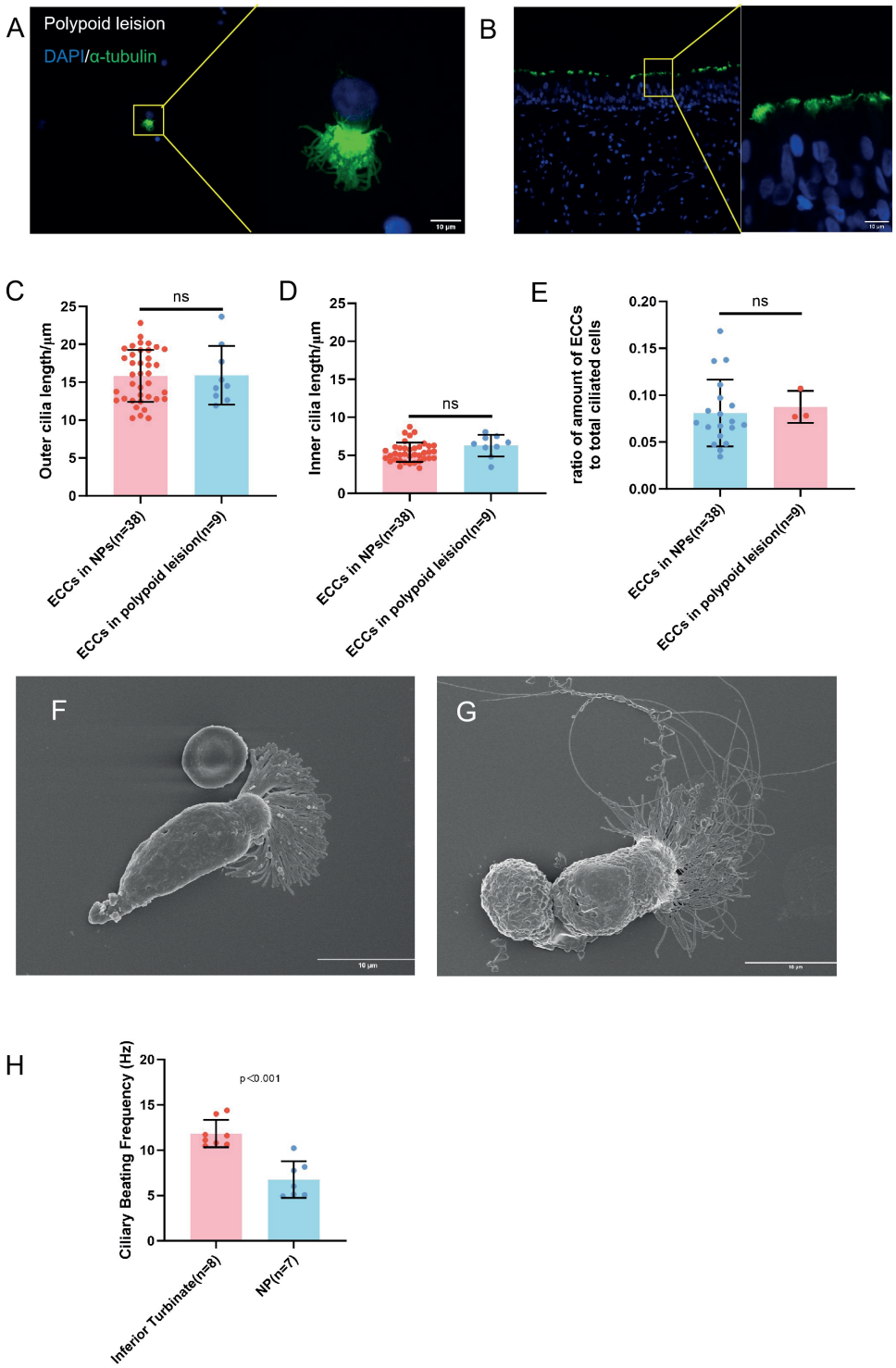

Figure 3. Elongated ciliated cells in polypoid-transformed lesions. (A, B) Representative IF images of α-tubulin (green), showing stratified and elongated ciliated cells (ECCs) in cytospin preparations and tissue sections from polypoid-transformed lesion. Nuclei are stained in blue (400× magnification; scale bars = 10 μm) (C, D) Comparisons of outer and inner cilia length between ciliated cells from NPs tissue (n = 38) and those from polypoid-transformed lesions (n = 9). Data are presented as mean ± SD. Statistical significance was determined by Student's t-test. All slides were evaluated at 400× magnification. (E) Comparison of the ratio of ECCs to total ciliated cells between the NPs and polypoid-transformed lesion groups. (F) Scanning electron microscopy (SEM) image of an inferior turbinate-derived ciliated cell from a non-CRSwNP patient, displaying regularly arranged cilia with uniform length and consistent diameter (SEM; 3,000× magnification). (G) SEM image of an NPs-derived ciliated cell, showing markedly elongated and disorganized cilia. Thicker cilia are visible near the cell periphery, while the outer long cilia progressively taper in diameter (SEM; 3,000×magnification). (H) Comparison of ciliary beat frequency between ciliated cells from NPs (n = 7) and inferior turbinate (non-CRSwNP) (n = 8) sources.

Corrected Proof

To determine the temporal emergence of elongated cilia in NPs pathogenesis, we further observed polypoid-altered mucosal tissues (n = 3), aiming to assess whether these unique cilia are present at the initial stage of polypoid transformation. There was also a distinct population of stratified, elongated cilia identified in these tissues (Figure 3A). IF imaging of fixed epithelium further revealed non-uniform ciliary morphology (Figure 3B), with a substantial subset of ciliated cells exhibited disordered architecture, manifesting as disorganized or sparse ciliary arrays, similar to NPs. The outer cilia demonstrated a distinct elongated and sparsely distributed morphology (15.91 ± 3.86 μm). In contrast, the inner cilia of ciliated cells exhibited morphological characteristics comparable to those observed in NPs-derived ciliated cells, displaying a short and thickened phenotype (6.28 ± 1.43 μm). Notably, no significant difference was found in either the outer cilia length of ECCs (comparing NPs and polypoid-transformed mucosa; Figure 3C) or their inner cilia length (Figure 3D). The proportion of ECCs among ciliated cells in polypoid-altered tissues (8.74% ± 1.71%) showed no difference compared to that in NPs (8.10% ± 3.55%, Figure 3E).

To better examine the morphology of these ECCs, isolated and uncultured hNECs were fixed with glutaraldehyde and prepared as cytospin slides for subsequent scanning electron microscopy (SEM). The SEM images revealed that, compared to typical ciliated cells (Figure 3F), these ECCs possessed longer, thinner, and more disorganized cilia that exhibited bending and twisting (Figure 3G). Since SEM is considered the gold standard for morphological assessment, these findings provide ultrastructural confirmation of the ECCs phenotype previously identified by IF.

Reduced ciliary beat frequency in nasal polyps-derived ciliated cells

To assess whether the function of ECCs was also altered, we measured the ciliary beat frequency (CBF) in hNECs derived from NPs and inferior turbinate (non-CRSwNP) tissues after ALI culture. CBF in NPs-derived ciliated cells (6.76 ± 2.01 Hz) was significantly lower than that in inferior turbinate-derived cells (11.84 ± 1.52 Hz, Figure 3H).

Notably, NPs epithelium contains a high proportion of ECCs. While technical limitations currently preclude direct, single-cell measurement of CBF specifically in ECCs, the concurrent findings of ECCs enrichment and global CBF reduction in NPs tissue raise the possibility that these structurally aberrant cilia may exhibit impaired motility. Direct functional assessment of ECCs at single-cell resolution remains an important goal for future studies.

Discussion

The nose is the primary airway entrance, equipped with protective filtration and mucociliary systems [14]. Embryologically, facial and nasal structures arise from the ectoderm, neural crest, and mesoderm [15]. Sinuses such as the frontal and sphenoidal develop mainly after birth, often maturing by the end of puberty [16]. Variations in anatomical location lead to differing exposure to external stimuli across nasal and sinus mucosa, which may result in regional differences in epithelial cell morphology.

The OMC is a critical drainage pathway for sinus mucus, and chronic obstruction or recurrent infection can lead to the development of CRSwNP [17]. Effective clearance within the nasal cavity and sinuses depends on the MCC system, which relies on functional cilia and mucus to maintain homeostasis and prevent such pathology [18], highlighting the importance of studying mucosal physiology, particularly within the OMC. Despite the recognized importance of MCC, regional heterogeneity in ciliary morphology, particularly the presence of structurally distinct ciliated cell populations, remains poorly characterized. In this study, we identified a distinct population of ECCs enriched in NPs epithelium, providing new insights into region- and disease-specific ciliary alterations in CRSwNP.

This study is the first to systematically examine ciliated cells across multiple sinonasal sites, including frontal sinus, ethmoid sinus, and maxillary sinus, sphenoid sinus, uncinate process and inferior turbinate in both CRSwNP patients and non-CRSwNP patients. Our IF analysis demonstrated that largely similar ciliary morphology and uniform cilia distribution in all mucosal regions except NPs. Cilia on pseudostratified columnar epithelium showed consistent length and structural continuity (Figure 1C). Analysis of hNECs revealed oval-shaped cells with cilia that were uniformly long and densely packed, arranged in a fan-like pattern away from the nucleus (Figure 1B). We further evaluated the structural differences in ciliated cells from different nasal mucosa through the $length_{VA}$, $length_{HA}$, ratio of $length_{HA}/length_{VA}$, cilia length, and cilia length/lengthVA ratio of the ciliated cells. Notably, cilia in NPs-derived cells were significantly elongated (8.17 ± 3.35 μm), exceeding the normal range of 5.0–7.0 μm [8]. In contrast, almost all the mucosa-derived cilia fell within the normal range. Therefore, we established a basis for subsequent research: the ECCs observed in NPs are likely driven by the disease itself rather than by anatomical location.

CRS involves abnormalities in nasal mucosal cilia, including cilia loss [19], irregularity, crowding, elongation [9] and functional impairment [10]. Previous studies typically compared NPs cilia only with those from the uncinate process [20] or inferior turbinate [21]. In contrast, we systematically mapped ciliary morphology across sinonasal sites, focusing on NPs-derived ciliated cells to define their specific pathology. Direct comparison between CRSwNP and non-CRSwNP sinus mucosa revealed distinctive hyperelongated cilia—a phenotype that has been previously described [9]. While previous studies have largely relied on ex vivo models, which may not fully recapitulate in vivo conditions, we directly obtained nasal mucosa tissues and employed optimized fixation methods to preserve native ciliary architecture. Beyond traditio-

Corrected Proof

nal length measurements, we assessed $length_{VA}$ and $length_{HA}$ of ciliated cells and found that the ratio of ciliary length to $length_{HA}$ also helps distinguish ECCs from other ciliated cells. Beyond their distinct morphology, ECCs also exhibited a disease-specific distribution pattern: their proportion was significantly higher in CRSwNP. Notably, the proportion of ECCs was significantly higher in CRSwNP (8.10% ± 3.55%) than in non-CRSwNP (1.08% ± 1.37%), suggesting ciliary hyperelongation may be a pathophysiological hallmark of NPs-related epithelial dysfunction. In summary, we hypothesize that cilia elongation may be driven by intrinsic and/or extrinsic stimuli, promoting abnormal proliferation and differentiation pathways.

Previous studies indicate that cilia damage in CRSwNP may result from viruses [12], bacteria [13], or inflammatory factors such as interleukin-4 [22], interleukin-6 [23], interleukin-17A [10]. A whole-transcriptome RNA sequencing study by Peng et al. [24] suggests that cilia function may be a key distinguishing feature of CRSwNP. Consistent with this, elongated ciliary structures are observed in polypoid-altered lesions, indicating that ciliary abnormalities may serve as an early biomarker in NPs pathogenesis. This supports the hypothesis that such lesions represent a transitional stage toward NPs formation, marked by persistent ciliary dysfunction, structural disorganization, and hyperelongation.

Furthermore, the identification of stratified ECCs in NPs holds significant clinical implications. These abnormal cilia may disrupt MCC, leading to mucus stasis, recurrent infection, and persistent inflammation - core features of CRSwNP. Targeting the pathways driving ciliary elongation could thus offer a novel therapeutic approach. Current biologics for CRSwNP (e.g., dupilumab, mepolizumab), which modulate type 2 inflammation, may indirectly affect ciliary structure and merit investigation for their morphological impact. Furthermore, the persistence of ECCs in polypoid-transformed mucosa and even after in vitro culture indicates that these cells may carry irreversible genetic or epigenetic alterations. If not eliminated during surgery, these abnormal progenitor cells could drive NPs recurrence. However, due to the lack of reliable observational methods, this finding was not reported in detail and requires further verification.

This study offers novel cilia observation and mucosal insights but is limited by small sample size, lack of NPs subtyping, and uninvestigated ECCs-associated pathways. Critically, the absence of CBF data from non-polyp mucosa in CRSwNP patients prevents us from distinguishing a localized polyp effect from a global mucosal impairment. Future studies with larger, subtyped cohorts and paired polyp/non-polyp samples are needed to validate our findings and to assess the potential of targeting elongated cilia as a treatment for NPs.

Conclusion

Through comprehensive mapping of ciliated cell morphology across sinonasal mucosa, we identified a distinct population of stratified ECCs in NPs. Notably, these aberrant ciliary features emerged as early as the polypoid lesion stage and persisted post-ALI culture, suggesting intrinsic, irreversible mutations of NPs-derived ciliated progenitor cells. Elucidating these mechanisms could unveil novel pathways driving NPs pathogenesis, highlighting their potential as early biomarkers or therapeutic targets.

Author contributions

All authors were involved in the study. Acquisition of data and analysis of data: H-YD, -RP and H-JQ. Interpretation of data: H-YD, and Q-TY. Drafts and revisions during the writing process: H-YD, M-RP, H-JQ and Q-TY. Revising the article and final approval of the article before submission: all authors.

Acknowledgments

The authors would like to thank all the participants and the Third Affiliated Hospital, Sun Yat-Sen University. This work was supported by the National Natural Science Foundation of China (Grant No. 82000957, 82401331, 82101197 and 82271148, 82571289).

Conflict of interest

The authors declare no competing interests.

Funding

No funding.

References

1. Lee RJ, Cohen NA. Innate immune function in chronic rhinosinusitis. J Allergy Clin Immunol 2025; 155(5):1472-1474.
2. Antunes MB, Gudis DA, Cohen NA. Epithelium, cilia, and mucus: their importance in chronic rhinosinusitis. Immunol Allergy Clin North Am 2009; 29(4):631-643.
3. Stevens WW, Lee RJ, Schleimer RP, Cohen NA. Chronic rhinosinusitis pathogenesis. J Allergy Clin Immunol 2015; 136(6):1442-1453.
4. Gudis D, Zhao KQ, Cohen NA. Acquired cilia dysfunction in chronic rhinosinusitis. Am J Rhinol Allergy 2012; 26(1):1-6.
5. Fokkens WJ, Lund VJ, Hopkins C, et al. European Position Paper on Rhinosinusitis and Nasal Polyps 2020. Rhinology 2020; 58(Suppl S29):1-464.
6. Rudmik L, Smith TL, Schlosser RJ, Hwang PH, Mace JC, Soler ZM. Productivity costs in patients with refractory chronic rhinosinusitis. Laryngoscope 2014; 124(9):2007-2012.
7. Bhattacharyya N, Orlandi RR, Grebner J, Martinson M. Cost burden of chronic rhinosinusitis: a claims-based study. Otolaryngol Head Neck Surg 2011; 144(3):440-445.
8. Houtmeyers E, Gosselink R, Gayan-Ramirez G, Decramer M. Regulation of mucociliary clearance in health and disease. Eur Respir J 1999; 13(5):1177-1188.
9. Li YY, Li CW, Chao SS, et al. Impairment of cilia architecture and ciliogenesis in hyperplastic nasal epithelium from nasal polyps. J Allergy Clin Immunol 2014; 134(6):1282-

Corrected Proof

1292.
10. Qiu H, Liu J, Wu Q, et al. An in vitro study of the impact of IL-17A and IL-22 on ciliogenesis in nasal polyps epithelium via the Hippo-YAP pathway. J Allergy Clin Immunol 2024; 154(5):1180-1194.
11. Bartosh Z, Aishwarya V, Hancock WW, Akimova T. New approaches to old techniques in cell handling for microscopy. Cells 2025; 14(16).
12. Wu CT, Lidsky PV, Xiao Y, et al. SARS-CoV-2 replication in airway epithelia requires motile cilia and microvillar reprogramming. Cell 2023; 186(1):112-130.e120.
13. Boase S, Jervis-Bardy J, Cleland E, Pant H, Tan L, Wormald PJ. Bacterial-induced epithelial damage promotes fungal biofilm formation in a sheep model of sinusitis. Int Forum Allergy Rhinol 2013; 3(5):341-348.
14. Geurkink N. Nasal anatomy, physiology, and function. J Allergy Clin Immunol 1983; 72(2):123-128.
15. Neskey D, Eloy JA, Casiano RR. Nasal, septal, and turbinate anatomy and embryology. Otolaryngol Clin North Am 2009; 42(2):193-205, vii.
16. Pohunek P. Development, structure and function of the upper airways. Paediatr Respir Rev 2004; 5(1):2-8.
17. Bachert C, Marple B, Schlosser RJ, et al. Adult chronic rhinosinusitis. Nat Rev Dis Primers 2020; 6(1):86.
18. Roth D, Şahin AT, Ling F, et al. Structure and function relationships of mucociliary clearance in human and rat airways. Nat Commun 2025; 16(1):2446.
19. Bizaki AJ, Numminen J, Taulu R, Kholova I, Rautiainen M. Treatment of rhinosinusitis and histopathology of nasal mucosa: A controlled, randomized, clinical study. Laryngoscope 2016; 126(12):2652-2658.
20. Lee SH, Han MS, Lee TH, et al. Rhinovirus-induced anti-viral interferon secretion is not deficient and not delayed in sinonasal epithelial cells of patients with chronic rhinosinusitis with nasal polyp. Front Immunol 2022; 13:1025796.
21. Xie X, Wang P, Jin M, et al. IL-1β-induced epithelial cell and fibroblast transdifferentiation promotes neutrophil recruitment in chronic rhinosinusitis with nasal polyps. Nat Commun 2024; 15(1):9101.
22. Fieux M, Carsuzaa F, Bellanger Y, et al. Dupilumab prevents nasal epithelial function alteration by IL-4 in vitro: Evidence for its efficacy. Int Forum Allergy Rhinol 2024; 14(8):1337-1349.
23. Bequignon E, Mangin D, Bécaud J, et al. Pathogenesis of chronic rhinosinusitis with nasal polyps: role of IL-6 in airway epithelial cell dysfunction. J Transl Med 2020; 18(1):136.
24. Peng Y, Zi XX, Tian TF, et al. Whole-transcriptome sequencing reveals heightened inflammation and defective host defence responses in chronic rhinosinusitis with nasal polyps. Eur Respir J 2019; 54(5).

Qintai Yang
Department of Otolaryngology Head and Neck Surgery
Department of Allergy
The Third Affiliated Hospital of Sun Yat-sen University
600 Tian He Road
Guangzhou
China 510630

Tel: + 86 20-85252239
Fax: +86 20-85252239
E-mail: yangqint@mail.sysu.edu.cn

Huijun Qiu
Department of Otolaryngology Head and Neck Surgery
Department of Allergy
The Third Affiliated Hospital of Sun Yat-sen University
600 Tian He Road
Guangzhou
China 510630

Tel: + 86 20-85252239
Fax: +86 20-85252239
E-mail: qiuhj7@mail.sysu.edu.cn

Huiyi Deng*, Mingrui Pan*, Qintai Yang#, Huijun Qiu#

Department of Otorhinolaryngology-Head and Neck Surgery, Department of Allergy, The Third Affiliated Hospital, Sun Yat-sen University, Guangzhou, China

*,# equal contribution

Rhinology 64: 4, 0 - 0, 2026
https://doi.org/10.4193/Rhin25.225

Received for publication:
April 25, 2025
Accepted: March 30, 2026

Associate Editor:
Sanna Toppila-Salmi

This manuscript contains online supplementary material

Corrected Proof

SUPPLEMENTARY MATERIAL

Materials and methods

Subjects and samples collection

This study was conducted in accordance with the Declaration of Helsinki. The study was approved by the hospital's ethics committee (Approval No. RG2023-124-01). All patients were informed of the purposes and procedures of the study and provided written informed consent. CRSwNP and non-CRSwNP patients (allergic rhinitis, fungal sinusitis, deviation of the nasal septum, optic nerve injury and pituitary tumor) were recruited from the Department of Otolaryngology from the Third Affiliated Hospital of Sun Yat-sen University in China. All patients were free of non-steroidal anti-inflammatory drugs-exacerbated respiratory disease (N-ERD) and did not have any other allergic diseases except for asthma and allergic rhinitis. All the CRSwNP patients included had no allergic rhinitis. All the non-CRSwNP patients included had no asthma. Patients with atopy were diagnosed positive with symptoms and allergen-specific IgE (sIgE) higher than 0.35 kUA/L tested by ImmunoCAP. Before the operation, all patients did not take any additional medication. The demographic information of the participated patients is shown in Table 1. The diagnosis of CRSwNP was established according to the criteria outlined in the European Position Paper on Rhinosinusitis and Nasal Polyps (EPOS) 2020 [1]. Biopsies of sinus mucosa were obtained during endoscopic sinus surgery (ESS), while inferior turbinate mucosa (IT) were obtained from healthy control subjects undergoing septoplasty. All the patients didn't have concurrent upper respiratory infections in four weeks, systemic diseases, or a history of nasal surgery. Additionally, none of the patients had used macrolides, glucocorticosteroids, antibiotics, or T2 biologics therapy within three months prior to the study that may affect cilia. CRSwNP was classified as eosinophilic when the average histologic count of eosinophils exceeded ten in high power fields (400× magnification) after hematoxylin-eosin (HE) staining.

Tissue fixation

Fresh nasal tissues from patients were soaked in 4% paraformaldehyde (PFA, Sigma-Aldrich, St. Louis, MO, USA), then washed by ethyl alcohol and xylene (Solarbio, Beijing, China), finally were embedded in paraffin and were made into sections.

Cytospin preparation

Cytospin slides were prepared by centrifuging cells onto glass slides to preserve cellular morphology for imaging [2]. Human nasal epithelial cells (hNECs) were dissociated by trypsinization (Gibco, Carlsbad, CA, USA) and fixed in 4% PFA at room temperature for 15 minutes, then washed three times with PBS for five minutes each time. Cytospin preparation (2×10^4 cells/slide) was created by spinning for five minutes at 500 rev/min on a Shandon Cytospin four Cytocentrifuge (Thermo Fisher Scientific, Waltham, MA, USA).

Immunofluorescent staining

The paraffin sections to be processed were placed on a roasting machine at 64°C for two hours, then were immersed in xylene and gradient alcohol (100% twice, 95% twice, 70% twice) for deparaffinization. Deparaffinized tissue slides and cytospins were repaired with 1×Tris-EDTA antigen recovery solution (pH 9.0, Servicebio, Wuhan, China) at 100°C for ten minutes, then removed the sections and allowed them to cool naturally to room temperature. The samples were closed off by 10% goat serum (Gibco, Carlsbad, CA, USA) for 30 min. The paraffin sections and hNEC slides were permeabilized with 0.1% Triton ×-100 for ten min. The primary antibody to characterize cilium is mouse anti-human alpha-tubulin monoclonal antibody (α-tubulin), purchased from Abcam (ab24610, Abcam, Cambridge, UK). The samples were incubated by primary antibodies at 4°C overnight (the dilution of antibody targeted to alpha-tubulin was 1:400), and then stained with goat anti-mouse Alexa Fluor 488 conjugated secondary antibodies (A3273, Thermo Fisher Scientific, Waltham, MA, USA) in the dark at room temperature for one hour; the samples were then stained with 4',6'- diamidino-2-phenylindole (DAPI) for visualization of the nuclei. Use Fluorescence microscope (Olympus, Tokyo, Japan) to take pictures and use NIS-Elements Viewer (5.21 64-bit, Nikon, Tokyo, Japan) to edit.

Human nasal epithelial cell culture

Primary epithelial cells were isolated from fresh nasal specimens. Fresh specimens were cut into pieces and processed by enzymatic digestion with Dispase II (Sigma-Aldrich, St. Louis, MO, USA) at 4°C overnight. The digested tissue suspension was again digested by trypsin (Sigma-Aldrich, St. Louis, MO, USA) and filtered by using 70 μm cell strainers (Corning, Corning, NY, USA) to obtain single-cell suspension. Human nasal epithelial cells (hNECs) were cultured in our previous progenitor cell culture system as reported [3]. The hNECs were then transferred to an ALI system to become fully differentiated ciliated cells within four weeks according to PneumaCult™-ALI Medium (Stemcell Technologies, Vancouver, BC, Canada) specification.

Measurement of cilia and cellular morphology

Image J (v1.8.0.345; NIH, Bethesda, MD, USA) was used to measure cell cilia length, the length of the cell parallel to the direction of cilia growth (defined as the horizontal axis, $length_{VA}$), and the length of the cell central perpendicular to the direction of

Corrected Proof

cilia growth (defined as the vertical axis, length$_{VA}$). Ten random fields were taken from each cell slide, and the measurements were repeated three times by three researchers to obtain the data. The researchers independently assessed all cases in a blind fashion to have a standardized histologic evaluation of the staining.

Measurement of ciliary beat frequency

Add 200 µL of pre-warmed (37°C) 1× dPBS to the ALI transwell, incubate for ten minutes, and then remove it. The transwell was then placed under a microscope (200× magnification) at room temperature. Ciliary Beat Frequency (CBF) was automatically analyzed using the Sisson-Ammons video analysis (SAVA) system (Ammons Engineering, Omaha, NE, USA). The system recorded one frequency value per field of view every 30 seconds over a continuous period of three min. For each experimental group, at least three independent random fields were recorded. The average CBF value was calculated for statistical analysis.

Scanning electron microscope

hNECs were fixed by Glutaraldehyde fixative and made into cytospin slides. The Cytospin-fixed cell slides were air-dried at room temperature and secured centrally on the sample stage of an ion sputter coater (Hitachi MC1000, Tokyo, Japan). After evacuating the chamber to high vacuum (approximately 5 × 10^{-1} Pa), argon was introduced to maintain a stable pressure of 20 Pa. A conductive gold layer approximately 5 nm thick was deposited on the sample surface by applying a set current between the cathode (gold target) and anode. The coated slides were then transferred to a scanning electron microscope (SEM, Hitachi SU8020, Tokyo, Japan). Under an accelerating voltage of 10 kV, regions of interest were located at low magnification. The magnification was gradually increased and focus along with astigmatism correction were alternately adjusted to acquire clear secondary electron images for analysis.

Statistics and reproducibility

All statistical analyses were performed using SPSS (version 29.0.2.0; IBM Corp., Armonk, NY, USA), and graphs were generated using GraphPad Prism (version 8.0; GraphPad Software, San Diego, CA, USA). Based on preliminary data, a sample size of 19–32 per group provided >80% power to detect a mean difference of 2.5 µm in cilia length with $\alpha = 0.05$. Between-group comparisons were performed using an unpaired Student's t-test (for two groups) or one-way ANOVA (for three or more groups). Results were reported as mean differences with 95% confidence intervals. When significant differences were found in multiple group comparisons, post-hoc pairwise tests with Bonferroni correction were conducted. A two-tailed p value of < 0.05 was considered statistically significant.

References

1. Fokkens WJ, Lund VJ, Hopkins C, et al. European Position Paper on Rhinosinusitis and Nasal Polyps 2020. Rhinology 2020; 58(Suppl S29):1-464.
2. Bartosh Z, Aishwarya V, Hancock WW, Akimova T. New approaches to old techniques in cell handling for microscopy. Cells 2025; 14(16).
3. Qiu H, Liu J, Wu Q, et al. An in vitro study of the impact of IL-17A and IL-22 on ciliogenesis in nasal polyps epithelium via the Hippo-YAP pathway. J Allergy Clin Immunol 2024; 154(5):1180-1194.